Binding of Natural Antioxidant, Curcumin with Metal-Salen Complexes

T. Rajendran[1,2], K. Senthil Murugan[3], G. Balakrishnan[3], C. Karthikeyan[3], S. Thanaraj[4], G. Arunkumar[4], V. K. Sivasubramanian[5], M. Ganesan[5], K. Vijaya[1]

[1]Professor, Department of Chemistry, PSNA College of Engineering & Technology, Dindigul-624 622, India.
[2]Associate Professor and Head (Rtd), Department of Chemistry, Vivekananda College, Tiruvedakam West, Madurai 625 234, India
[3]Research Scholar, Department of Chemistry, Vivekananda College, Tiruvedakam West, Madurai 625 234, India.
[4]P.G. Student, Department of Chemistry, Vivekananda College, Tiruvedakam West, Madurai, 625 234, India.
[5]Associate Professor, Department of Chemistry, Vivekananda College, Tiruvedakam West, Madurai 625 234, India

Abstract- Six transition metal-salen complexes (metal = Fe, Mn and Cr) **1-6** have been synthesized and characterized using different spectroscopic and electrochemical techniques. The binding studies of natural antioxidant, curcumin with the complexes (**1-6**) have been carried out by electronic absorption spectroscopic technique. The substantial shift in the absorption maximum of complexes (**1-6**) when they bind to curcumin indicated that there was a strong binding between them. The binding constant calculated ranges from 20 to 2.46 X 10^4 M^{-1} s^{-1}. To the best of our knowledge, this is the first report for studying binding nature of curcumin, the natural antioxidant with these biologicallly relevant metal-salen complexes.

Index Terms- metal-salen complexes; anti-oxidant; binding constant; curcumin; UV-vis titration.

I. Introduction

Salicylidene-ethylenediamines, commonly known as salens, can stabilize the high oxidation states of most of the transition metals and even some p-block metals in various oxidation states and their complexes are capable of oxidizing a variety of organic compounds [1,2]. Because of their easily tunable chiral environment, metal-salen derivatives are efficient asymmetric catalysts for sulfoxidation [3-5], epoxidation [6], epoxide ring opening [7], hydrolytic kinetic resolution [8], hetero Diels-Alder reactions [9] etc., Mn(salen) complexes are widely utilized as highly reactive epoxidation catalysts [10-13]. Fe(salen) complexes serve as nonheme enzyme models to explore the oxidizing intermediates when activated by chemicals [14]. Recently Mellah et al. reported the efficient electropolymerized chromium–salen complexes for heterogeneous asymmetric catalysis [15]. Fujii et al. have made a detailed mechanistic study using sterically hindered manganese-salen complex as a model system to explore the structure–reactivity relationships for the high catalytic activity of the epoxidation catalyst, Mn(III)-salen [16].

As a principal curcuminoid, curcumin derived from the plant Curcuma longa, is a gold-colored spice commonly used for hundreds of years in Asian countries, not only for health care but also for the preservation of food and as a yellow dye for textiles [17]. Since the time of Ayurveda (1900 bc) turmeric has been used as chemotherapeutic agent for a wide variety of diseases including those of the skin, pulmonary, and gastrointestinal systems, aches, pains, wounds, sprains, and liver disorders. From the past five decades, extensive research has come to a conclusion that most of these activities associated with turmeric, are due to curcumin. Because of antioxidant nature of curcumin [18-19], it serves as anticancer drugs [20-23], anti-inflammatory [24,25], anti HIV [26], antibacterial and antifungal activities and thus has a potential against various malignant diseases, diabetes, allergies, arthritis, Alzheimer's disease [27-29], and other chronic illnesses. These effects are mediated through the regulation of various transcription factors, growth factors, inflammatory cytokines, protein kinases, and other enzymes. From a chemical stand point, the biological activities of curcumin are derived from the antioxidant property of the methoxyphenol group and the action of the aryl group in diketone [30-32]. β-diketones are present as the enol form, and form chelates with different transition metal ions, for example, Fe^{2+}, Fe^{3+}, Cu^{2+} and Zn^{2+} etc., [33-39]. It is desirable to study the nature of interaction between catalytic metal – salen complexes with curcumin. As far as we know, there is no literature available on the catalytic role of biologically relevant metal-salen complexes for the binding of biologically important curcumin (polyphenols). To accomplish this we have synthesized various metal– salen complexes (**1-6**).

II. Experimental Methods

2.1 Materials and Methods

All the chemicals were purchased from Aldrich and used as received. Some of them were from Merck. All the solvents and reagents, if necessary, were purified before use as per the standard procedures [40]. Complexes **1-6** were prepared from the previously published reports [41-43]. Electronic absorption spectra were measured with a JASCO V-530 UV-vis. Spectrophotometer. Thermostated temperature bath was used to maintain the required temperature. The infrared spectra of the complexes were recorded in a JASCO FT/IR-430 spectrophotometer in KBr pellet medium. Electrochemical measurements were carried out on a potentiostat-galvanostat (CH Instruments Electrochemical Analyzer) using a 3 mm^2 surface glassy carbon electrode as the working electrode, a platinum wire as the counter electrode, and a standard calomel electrode as the reference electrode. The acetonitrile solution of complexes (1 mM) along with the electrolyte (0.10 M of sodium

perchlorate) was purged with nitrogen for about twenty minutes before the electrochemical measurements.

2.2 Evaluation of molar extinction coefficient

In spectrophotometry, the intensity of the incident light (I_o), the intensity of the transmitted light (I), the concentration of the solution (C), the path length of the beam of light within the solution (l) and molar extinction coefficient (ε) which is characteristic of the absorbing substance are related by the Beer-Lambert Law as:

$$I = Io \exp(\varepsilon.C.l)$$

Absorbance or optical density (OD) = $\log I/Io = \varepsilon.C.l$

The instrument gives the optical density directly. By substituting the values of 'C' and 'l' the molar extinction coefficient (ε) can be calculated.

III. Results and Discussion

The structures metal-salen complexes (metal = Fe, Mn, Cr) **1-6** and curcumin are shown in Figure 1.
(Insert Figure 1)

3.1. Characterization by UV-Vis spectral techniques

The absorption spectrum of complex **4** (Figure 2, left) shows a broad band at 463 nm, a shoulder at 299 nm and a sharp peak at 258 nm. The peak at 463 nm is assigned to the LMCT transition and those at 299 nm and 258 nm are assigned to the π-π* transitions [41-43]. The LMCT absorption maximum is sensitive to the nature of the substituent in the salen ligand (Table 1). The parent iron(III)-salen complex shows characteristic absorption at λ_{max} = 470 nm. Introduction of an electron with drawing 5-NO_2 group shifts the λ_{max} value from 470 to 463 nm. The other complexes show π-π* transitions at 200-300 nm and LMCT transition at 400-475 nm similar in both size and shape. Curcumin in acetonitrile (Figure 2, right) shows three strong absorption bands at 248, 298 and 416 nm. The binding of curcumin with complexes (**1-6**) is inferred from the change in the shape of the LMCT absorption of complex and a substantial shift in the λ_{max} value during the incremental addition of curcumin to metal-salen complexes (Tables 3-8).
(Insert Figure 2 and Table 1)

3.2. Characterization by IR – Spectral techniques

The infrared spectra of the complexes were collected in Table 2. The ν^{-1} (C= O) band at 1252 cm^{-1} and ν^{-1}(H-C=N) band at 1633 cm^{-1} were found for complex **4** [42]. Similar values were also obtained for other complexes (see ESI).
(Insert Table 2)

3.3. Cyclic voltammetric studies

The electrochemical properties of complexes **1-6** were collected in Table. 1 and are in accordance with our previously published data [42].

3.4. Binding studies of curcumin with metal-salen complexes

The binding constant can be calculated using the following equation.

$$\frac{[Complex][Substrate]}{\Delta A} = \frac{[Complex] + [Substrate]}{\Delta \varepsilon} + \frac{1}{K_b . \Delta \varepsilon}$$

Where,

ΔA = difference absorption in presence and absence of substrate
$\Delta \varepsilon$ = difference in extinction coefficient
K_b = binding constant

The binding constants calculated were in the range from 20 to 2.46 X 10^4 (Tables 3-8) for the interaction of curcumin with different metal-salen complexes (**1-6**). The enormous increase in the binding constants revealed the fact that the well known catalyst, Fe(salen) binds extensively with the curcumin in acetonitrile medium. As per the observations of Zsila et.al [44], the binding behaviour may be due to the interaction of curcumin in the keto-enol form. In order to check the influence of the electronic effect on the binding phenomenon, the binding constants were calculated for Fe-Cl salen (**2**) using UV-vis titrations. To our surprise the binding constant values remain constant in the range 56-101. The chloro substitution on the salen moiety retards the binding to the tune of three orders. Also the UV-vis titrations explicitly reveal the fact that the electron donating nature of methyl moiety in the 5 and 5' positions retards the binding due to the accumulation of negative charge on the central metal atom. Due to the enhanced negative charge on the binding site, the electron donating groups in salen part renders less binding. This was substantiated by the observed binding constant in the range 20 to 59. An interesting thing is the chloro substitution should enhance the binding on the basis of the reactivity principle. Rather it retards the binding (K_b = 56-101). This may be explained by the domination of the electronic factor rather than the inductive effect.
(Insert Figure 3)

Further checking was carried out by the UV-visible titration of Fe-nitrosalen complex (**4**) with curcumin. The result showed enhanced binding constant values in the range 4.2 X 10^3 to 4.9 X 10^3. This elevated value proved the dominant effect of electron withdrawing group on the binding phenomenon. The UV-visible binding studies paved a new path to understand the novel binding mechanism of the well known biologically important anticancer reagent, curcumin and the biocatalyst Fe-salen complex. To get an idea about the role of protic solvent on the binding, we have carried out a sample UV-visible titration with Fe-Cl salen-curcumin system in ethanolic medium. The expected hydrogen

bonding and enhanced polarity actually increases the binding by almost one order. i.e. the binding constant value ranges from 120 to 670 (56-100 in acetonitrile).
(Insert Tables 3-8)

3.5. Role of central metal ion in the binding behaviour

Curcumin and manganese complex of curcumin offer protective action against vascular dementia by exerting antioxidant activity. Hence changing the central atom of the Metal-salen complex will be an interesting study in the said binding behaviour. We have systematically changed the Fe^{III}–d^5 system by Mn^{III}–d^4 system. The binding behaviour of the Mn-salen complex with curcumin exhibits almost a similar behaviour. The binding constants were in the range of 3.0 X 10^3 to 4.6 X 10^3 (due to the poor solubility of the Mn-salen complex in acetonitrine, ethanol was used as solvent). The shoulder at 409 of the Mn-salen complex (**5**) gradually shifts from 394 nm to 425 nm on the subsequent addition of curcumin. The interesting observation is the λ_{max} of Mn-salen finally merges with the λ_{max} (423nm) of curcumin. Hence a change in the metal ion system does not show a marked change in the binding behaviour. A further insight was attempted by changing the Fe^{III}-d^5 system to Cr^{III}-d^3 system. The binding behaviour of Cr-salen (**6**) with curcumin reveals almost a similar behaviour. The binding constants were found to be in the range of 2.6 X 10^3 to 4.5 X 10^3 which shows a closer resemblance to that of Mn-salen –curcumin system. Hence a change in the central metal ion does not have a prominent role in the binding behaviour.

3.6. Probable Mechanism

The iron salen complex has its absorption maximum at 470 nm, whereas curcumin at 417 nm in acetonitrile. On the addition of curcumin, [2×10^{-6} M] the λ_{max} of the iron-salen complex (I) shifts to 460 nm, whereas the absorption peaks at 299 nm and 258 nm remains unchanged. Subsequent addition of curcumin (4×10^{-6}M) leads to further hypsochromic shift in the absorption maximum i.e, 441 nm. Incremental addition of curcumin changes the absorption maximum to 393 nm (10×10^{-6}M). Further addition increases the absorbance only keeping the λ_{max} almost constant. There is a shift of 77 nm is the absorption maximum of the iron-salen complex on the incremental addition of curcumin. The shifting of λ_{max} absorption towards the higher energy side (blue shift) is the evidence for the extensive binding of curcumin with the complex. We can explain the binding and blue shift in the absorption maximum of the iron-salen complexes in line with Zsila et al. [44]. He mentioned when curcumin binds to Human Serum Albumin (HSA) its two halves rotate around the central methylene group. It is a general concept that a blue shift in the absorption maximum is due to the formation of species with constrained geometry.

In a similar way the binding studies of methyl salen complex reveal the fact that the λ_{max} of the complex shifts from 486 nm to 440 nm on the addition of 2×10^{-6} M curcumin. It further shifts to 415 nm on further addition of curcumin. Continuous titration of curcumin with increasing concentrations exhibits an interesting binding phenomenon. A total of 71 nm shift is observed in this case. It is well documented that, due to its β-diketone moiety, curcumin exists entirely in the enol form with a trans-geometry both in solid state [45] and solution [46-48]. Thus, in this planar geometry the π-systems of the two feruloyl chromophores are allowed to interact with each other via the central, sp^2 - hybridized carbon atom resulting in a common conjugated π-system [49,50]. Yellow coloured acetonirtrile solutins of curcumin exhibit an intense, round-shaped absorption band centerd at 417 nm in acetonitrile, this band shows a characteristic vibrational fine structure which resembles the spectra of fully conjugated linear molecules such as carotenes and carenoids [49]. It should be emphasized that the visible absorption band of cucumin stems from a π-π* transition and not from an n-π* one as stated by Balasubramanian based on theoretical calculations [51]. Most likely, the weak, electronic dipole forbidden n→π* band is located somewhere under the main absorption band. Based on experimental data, several investigators suggested the first excited state of curcumin is highly polar due to intramolecular charge transfer from the phenyl ring towards the carbonyl moiety [48-50]. It was reported, when curcumin binds to Fe-salen complex its two halves rotate around the central methylene group. Such rotation, however, decreases or completely cancels π-conjugation between the two feruloyl parts, so the absorption maximum should shift below 400 nm, as in the case of cucumin derivates bearing a bulky substituent at the central methylene atom [52].

IV. Acknowledgement

We thank the Principal, the Management and the Head of the Department of Chemistry, Vivekananda College, Tiruvedakam West, Madurai, India for providing all the facilities to carry out this research work. The Principal, the Management and the Head of the Department of Chemistry of PSNA College of Engineering & Technology, Dindigul-624 622, India are sincerely acknowledged for their support.

V. Conclusion

Six Metal-salen complexes (Metal-Fe, Mn and Cr) have been synthesized and characterized by using UV-visible, IR and CV techniques. The binding studies with the curcumin revealed the fact that there is a strong interaction (binding) between the complexes **1-6** and curcumin. The binding constants calculated ranges from 20 to 2.5 X 10^4. Further a shift in the absorption maximum of the Fe-salen complex to the higher energy side to the tune of 77 nm (hypsochromic effect) is an indication of the binding. A change in the central transition metal ion (Fe, Mn, Cr) also insists the same binding behavior. A change in the polarity of the solvent in some specific cases also revealed the expected trend in the binding nature.

References

[1] Larrow, J.F.; Jacobsen, E.N. Asymmetric Processes Catalyzed by Chiral (Salen)Metal Complexes. Topics Organomet. Chem. 6, 123–152 (2004).

[2] Zulauf, A.; Mellah, M.; Hong, X.; Schulz, E. Recoverable chiral salen complexes for asymmetric catalysis: recent progress. Dalton Trans. 39, 6911–6935 (2010).

[3] Choi, J.Y.; Hwang, G.S.; Senapati, B.K.; Ryu, D. H. Efficient Asymmetric Sulfoxidation by Chiral Salen-Mn(III) Complexes. Bull. Korean Chem. Soc. 29, 1879- 1880 (2008).

[4] Gao, A.; Wang, M.; Shi, J.; Wang, D.; Tian, W.; Sun, L. Asymmetric oxidation of sulfides catalyzed by chiral (salen)Mn(III) complexes with a pyrrolidine backbone. Appl. Organometal. Chem. 20, 830–834 (2006).

[5] Schoumacker, S.; Hamelin, O.; Pecaut, J.; Fontecave, M. Catalytic Asymmetric Sulfoxidation by Chiral Manganese Complexes: Acetylacetonate Anions as Chirality Switches. Inorg. Chem. 42, 8110-8116 (2003).

[6] Xu, D.; Wang, S.; Shen, Z.; Xia, C.; Sun, W. Enantioselective oxidation of racemic secondary alcohols catalyzed by chiral Mn(III)-salen complexes with N-bromosuccinimide as a powerful oxidant. Org. Biomol. Chem. 10, 2730 (2012).

[7] Dioos, B.M.L.; Jacobs, P.A. Impregnation of dimeric CrIII(salen) on a silica and its application in epoxide asymmetric ring opening reactions. Applied Catalysis A: General. 282, 181-188 (2005).

[8] Zheng, X.; Jones, C. W.; Weck, M. Poly(styrene)-Supported Co–Salen Complexes as Efficient Recyclable Catalysts for the Hydrolytic Kinetic Resolution of Epichlorohydrin. Chem. Eur. J. 12, 576-583 (2006).

[9] Mellah, M.; Ansel, B.; Patureau, F.; Voituriez, A.; Schulz, E. Electropolymerized Cr–salen complexes for the heterogeneous asymmetric hetero Diels-Alder reaction. Journal of Molecular Catalysis A: Chemical. 272, 20-25 (2007).

[10] Srinivasan, K.; Michaud, P.; Kochi, J.K. Epoxidation of olefins with cationic (salen)manganese(III) complexes. The modulation of catalytic activity by substituents. J. Am. Chem. Soc. 108, 2309–2320 (1986).

[11] Zhang, W.; Loebach, J. L.; Wilson, S. R.; Jacobsen, E.N. Enantioselective epoxidation of unfunctionalized olefins catalyzed by salen manganese complexes. J. Am. Chem. Soc. 112, 2801–2803 (1990).

[12] Irie, R.; Noda, K.; Ito, Y.; Katsuki, T. Enantioselective epoxidation of unfunctionalized olefins using chiral (salen)manganese(III) complexes.Tetrahedron Lett. 32, 1055–1058 (1991).

[13] McGarrigle, E. M.; Gilheany, D. G. Chromium- and Manganese-salen Promoted Epoxidation of Alkenes. Chem. Rev. 105, 1563–1602 (2005).

[14] Kurahashi, T.; Kobayashi, Y.; Nagatomo, S.; Tosha, T. Kitagawa, T. Fujii, H. Oxidizing Intermediates from the Sterically Hindered Iron Salen Complexes Related to the Oxygen Activation by Nonheme Iron Enzymes. Inorg. Chem. 44, 8156-8166 (2005).

[15] Zulauf, A.; Hong, X.; Brisset, F.; Schulz, E.; Mellah. M. Electropolymerization of chiral chromium–salen complexes: new materials for heterogeneous asymmetric catalysis. New. J. Chem. 36, 1399–1407 (2012).

[16] Kurahashi, T.; Kikuchi, A.; Tosha, T.; Shiro, Y.; Kitagawa, T.; Fujii, H. Transient Intermediates from Mn(salen) with Sterically Hindered Mesityl Groups: Interconversion between MnIV-Phenolate and MnIII-Phenoxyl Radicals as an Origin for Unique Reactivity. Inorg. Chem. 47, 1674-1686 (2008).

[17] Cousins, M.; Adelberg, J.; Chen, F. Antioxidant capacity of fresh and dried rhizomes from four clones of turmeric (Curcuma longa L.) grown in vitro. Ind. Crop. Prod. 25, 129−135 (2007).

[18] Masuda T., Hidaka K., Shinohara A., Maekawa T., Takeda Y., Yamaguchi H. Chemical studies on antioxidant mechanism of curcuminoid: analysis of radical reaction products from curcumin. J. Agric. Food Chem, 47, 71-77 (1999).

[19] Motterlini R., Foresti R., Bassi R., Green C.J. Curcumin, an antioxidant and anti-inflammatory agent, induces heme oxygenase-1 and protects endothelial cells against oxidative stress. Free Radical Biol. Med. 281, 303-1312 (2000).

[20] Naama, J.H.; Al-Temimi, A.A.; Al-Amiery, A.A.H. African Journal of Pure and Applied Chemistry. 4, 68-73 (2010).

[21] Aggarwal B.B.,; Kumar A.; Bharti A.C. Anticancer potential of curcumin: preclinical and clinical studies. Anticancer Res. 23, 363–398 (2003).

[22] Anto R.J.; Kuttan G.; Dinesh Babu K.V.; Rajasekharan K.N.; Kuttan R. Antitumour and free radical scavenging activity of synthetic curcuminoids. Int. J. Pharm, 131, 1-7 (1996).

[23] Iqbal M.; Sharma S.D.;Okazaki Y.; Fujisawa M.; Okada S. Dietary Supplementation of Curcumin Enhances Antioxidant and Phase II Metabolizing Enzymes in ddY Male Mice: Possible Role in Protection against Chemical Carcinogenesis and Toxicity. Basic and Clinical Pharmacology&Toxicology. 92, 33-38 (2003).

[24] Huang M.T.; Lysz T.; Ferraro T.; Abidi T.F.; Laskin J.D.; Conney A.H. Inhibitory effects of curcumin in vivo lipoxygenase and cyclooxygensase activities in mouse epidermis. Cancer Res. 51, 813–819 (1991).

[25] Anto R.J.; Kuttan G.; Babu K.V.D.; Rajasekharan K.N.; Kuttan R. Antiinflammatory Activity of Natural and Synthetic Curcuminoids. Pharm. Pharmacol. Commun, 4, 103-106 (1998).

[26] Cohly, H.H.P.; Asad, S.; Das, S.K.; Angel, M.F.; Rao, M. Curcumin and dehydrozingerone derivatives: synthesis, radio labeling, and evaluation for beta-amyloid plaque imaging. Int. J. Mol. Sci. 4, 22-33 (2003).

[27] Ryu, E.K.; Choe, Y.S.; Lee, K.-H.; Choi, Y.; Kim, B.-T. Curcumin and Dehydrozingerone Derivatives: Synthesis, Radio labeling, and Evaluation for β-Amyloid Plaque Imaging. J. Med. Chem. 49, 6111-6119 (2006).

[28] Mazumdar A.; Raghvan K.; Weinstein J.; Kohn K.W.; Pommer Y. Inhibition of human immunodeficiency virus type-1 integrase by curcumin. Biochem. Pharmacol, 49, 1165–1170 (1995).

[29] Mishra, S.; Palanivelu, K. The effect of curcumin (turmeric) on Alzheimer's disease: An overview. Ann. Indian Acad. Neurol. 11, 13–19 (2008).

[30] Jovanovic S.V.; Boone, C.W; Steenken, S.; Trinoga, M.; Karskey, R.B. How curcumin works preferentially with water soluble antioxidants. J. Am. Chem. Soc. 123, 3064-3068 (2001).

[31] Sun, Y.M; Zhang, H.Y.; Chen, D.Z.; Liu, C.B. Theoretical elucidation on the antioxidant mechanism of curcumin: a DFT study. Organic Lett, 4, 2909-2911 (2002).

[32] Anto, R.J.A.; Mukhopadhyay, A.; Denning, K.; Aggarwal, B.B. Curcumin (diferuloylmethane) induces apoptosis through activation of caspase-8, BID cleavage and cytochrome c release: its suppression by ectopic expression of Bcl-2 and Bcl-xl. Carcinogenesis, 23, 143-150 (2002).

[33] Kumar, Y.; Garg, A.; Pandey, R. Study of Fe2+-Curcumin Complex by Polarogaphy. International Journal of Research in Pharmaceutical and Biomedical Sciences. 3, 1355- 1359 (2012).

[34] Jiao, Y.; Wilkinson, J.; Pietsch, E. C.; Buss, J.L.; Wang, W.; Planalp, R.; Trott, F. M.; Trotti, S.V. Iron chelation in the biological activity of curcumin. Free Radic. Biol. Med., 40, 1152-1160 (2006).

[35] Jiao, Y.; Wilkinson, J.; Di, X.; Wang, W.; Hatcher, H.; Kock, N.D.; Agastino, R.D.; Knovich, M.A.; Troti, F.M.; Troti, S.V. Curcumin, a cancer chemopreventive and chemotherapeutic agent, is a biologically active iron chelator. Blood. 113, 462-469 (2009).

[36] Hileti, D.; Panayiotodis, P.; Hoffbrand A.V. Iron chelators induce apoptosis in proliferating cells. J. Haematology. 89, 181-187 (1995).

[37] Miyamoto, D.; Endo, N.; Oku, N.; Arima, Y.; Suzuki, T.; Suzuki, Y. β-Thujaplicin zinc chelate induces apoptosis in mouse high metastatic melanoma B16BL6 cells. Biol. Pharm. Bull. 21, 1258-1262 (1998).

[38] Ishihara, M.; Sakagami, H. in vivo. Re-evaluation of Cytotoxicity and Iron Chelation Activity of Three,-Diketones by Semiempirical Molecular Orbital Method. 19, 119-124 (2005).

[39] Zhao, X.-Z.; Jiang, T.; Wang, L.; Yang, H.; Zhang, S.; Zhou, P. Interaction of curcumin with Zn(II) and Cu(II) ions based on experiment and theoretical calculation. J. Molec. Str. 984, 316–325 (2010).

[40] Furniss, B. S.; Hanooford, A. J.; Smith, P.W.G.; Tatchell, A. R. Vogel's text book of organic practical chemistry, 5th edn., Longman Scientific & Technical, New York (1989).

[41] Premsingh, S.; Venkataramanan, N. S.; Rajagopal, S.; Mirza, S. P. Vairamani, M.; Rao, P.S.; Velavan, K. Electron Transfer Reaction of Oxo(salen)chromium(V) Ion with Anilines. Inorg. Chem. 43, 5744-5753 (2004).

[42] Sivasubramanian, V.K.; Ganesan, M.; Rajagopal, S.; Ramaraj, R. Iron(III)-Salen Complexes as Enzyme Models: Mechanistic Study of Oxo(salen)iron Complexes- Oxygenation of Organic Sulfides. J. Org. Chem. 67, 1506-1514 (2002).

[43] Chellamani, A.; Alhaji, N.M.I.; Rajagopal, S.; Applicability and mathematical verification of the reactivity–selectivity principle in the oxidation of thioanisoles by oxo(salen)manganese(V) complexes. J. Chem. Soc., Perkin Trans. 2. 299-302 (1997).

[44] Zsila, F.; Bikadi, Z.; Simonyi, M. Unique, pH-dependent biphasic band shape of the visible circular dichroism of curcumin–serum albumin complex. Biochem. Biophys. Res. Commun. 301, 776-782 (2003).

[45] Payton, F.; Sandusky, P.; Alworth, W.L. NMR Study of the Solution Structure of Curcumin. J. Nat. Prod.70, 143–146 (2007).

[46] Roughley, P.J.; Whiting, D.A. Experiments in the biosynthesis of curcumin. J. Chem. Soc. Perkin Trans. 1. 69, 2379-2388 (1973).

[47] Arrieta, A.; Beyer, L.; Kleinpeter, E.; Lehmann, J.; Dargatz, M. Synthese und 1H-NMR-spektroskopische Untersuchungen neuer Curcuminanaloga. J. Prakt. Chem. 334, 696-700 (1992).

[48] Khopde, S.M.; Priyadarsini, K.I.; Palit, D.K.; Mukherjee, T. Effect of solvent on the excited-state photophysical properties of curcumin. Photochem. Photobiol. 72, 625-631 (2000).

[49] Chignell, C.F.; Bilski, P.; Reszk, K.J.; Motten, A.G.; Sik, R. H.; Dahl, T. A. Spectral and photochemical properties of curcumin. Photochem. Photobiol. 59, 295-302 (1994).

[50] Bong, P. H. Spectral and Photophysical Behaviors of Curcumin and Curcuminoids. Bull. Korean. Chem. Soc. 21, 81-86 (2000).

[51] Balasubramanian, K. Theoretical calculations on the transition energies of the UV–visible spectra of curcumin pigment in turmeric. Indian J. Chem., Sect. A 30, 61–65(1991)

[52] Pedersen, U.; Ramussen, P. B.; Lawesson, S. Synthesis of naturally occurring curcuminoids and related compounds. Liebigs. Ann. Chem. 12, 1557-1569 (1985).

AUTHORS

First Author – T. Rajendran, Professor, Department of Chemistry, PSNA College of Engineering & Technology, Dindigul-624 622, India.
Second Author – K. Senthil Murugan, Research Scholar, Department of Chemistry, Vivekananda College, Tiruvedakam West, Madurai 625 234, India.
Third Author – G. Balakrishnan, Research Scholar, Department of Chemistry, Vivekananda College, Tiruvedakam West, Madurai 625 234, India.
First Author – C. Karthikeyan, Research Scholar, Department of Chemistry, Vivekananda College, Tiruvedakam West, Madurai 625 234, India.
Second Author – S. Thanaraj, P.G. Student, Department of Chemistry, Vivekananda College, Tiruvedakam West, Madurai 625 234, India.
Third Author – G. Arunkumar, P.G. Student, Department of Chemistry, Vivekananda College, Tiruvedakam West, Madurai 625 234, India.
First Author – V. K. Sivasubramanian, Associate Professor, Department of Chemistry, Vivekananda College, Tiruvedakam West, Madurai 625 234, India
Second Author – M. Ganesan, Associate Professor, Department of Chemistry, Vivekananda College, Tiruvedakam West, Madurai 625 234, India
Third Author – K. Vijaya, Professor, Department of Chemistry, PSNA College of Engineering & Technology, Dindigul-624 622, India.

Correspondence Author – T. Rajendran, trajan602012@gmail.com , Tel.: +91-451-2554032 Fax: +91-451-2554249

Figures:

Figure 1.

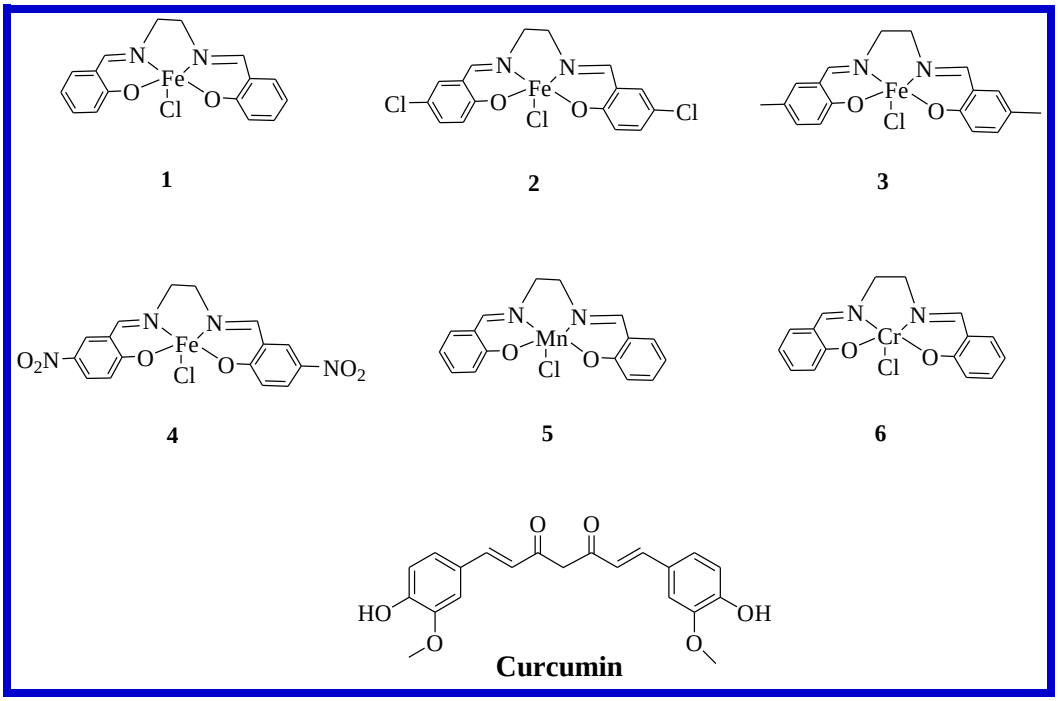

Figure 2.

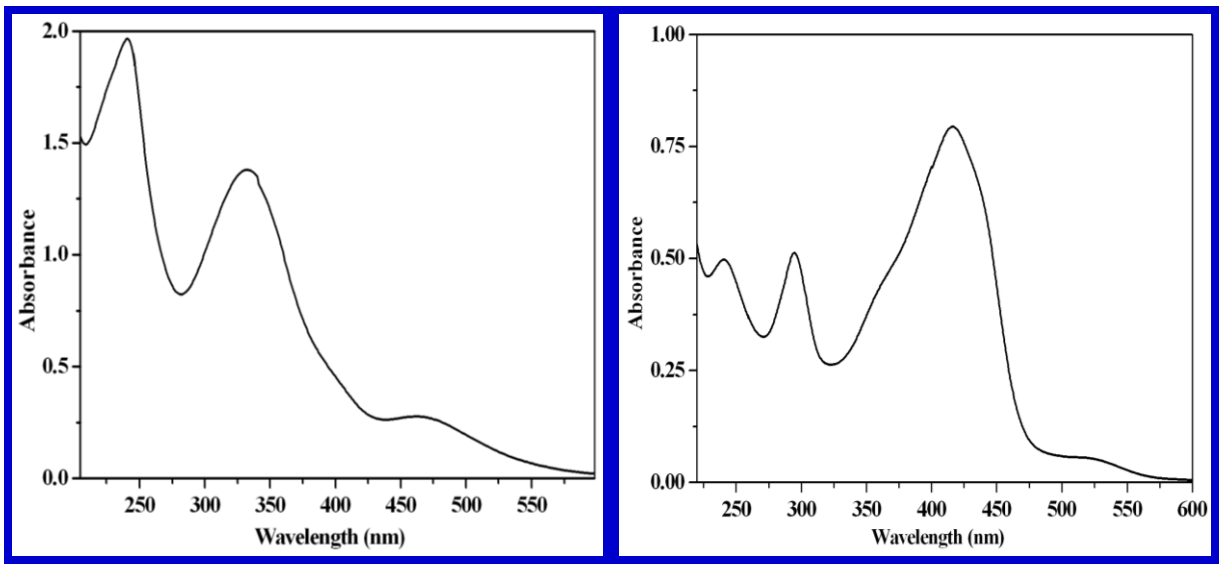

Figure 3.

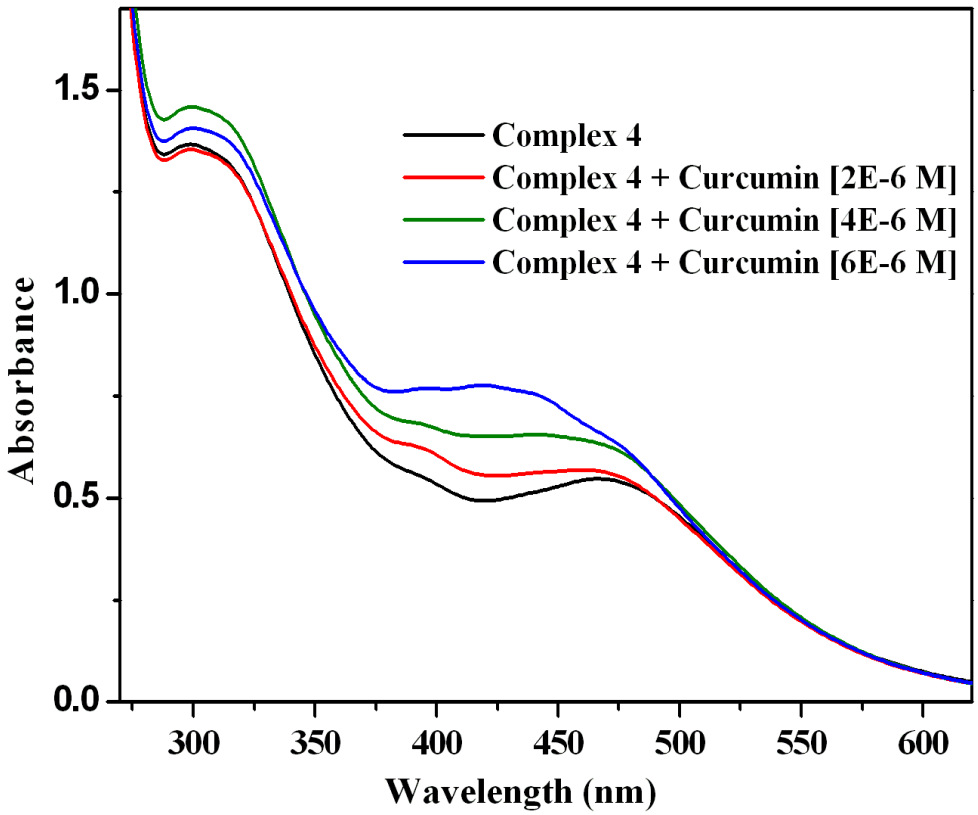

Tables:

Table 1.

S.No	Complex	λ_{max}, nm	$E_{1/2}$, V (vs. SCE)
1.	Complex **1**	470	-0.28
2.	Complex **2**	470	-0.24
3.	Complex **3**	468	-0.30
4.	Complex **4**	463	-0.15
5.	Complex **5**	409 (sh)	-
6.	Complex **6**	415	0.44[a]

[a]Reported E_{red} value.[41]

Table 2.

S.No	Complex	Stretching frequency, ν^{-1} (cm^{-1})
1.	Complex **1**	3636, 3543, 1639, 1621, 1293.
2.	Complex **2**	3639, 3599, 3554, 1987, 1635, 1552, 1180, 623.
3.	Complex **3**	3666, 3635, 3557, 1636, 1293, 1228, 862.

Table 3.

S.No	[Complex] (in mol L^{-1})	[curcumin] (in mol L^{-1})	λ_{max} (nm)	$10^{-5}\varepsilon_{max}$	$10^{-3}K_b$
1.	2 X 10^{-4}	2 X 10^{-6}	460	2.8	2.10
2.	2 X 10^{-4}	4 X 10^{-6}	441	1.6	10.30
3.	2 X 10^{-4}	6 X 10^{-6}	418	1.1	14.70
4.	2 X 10^{-4}	8 X 10^{-6}	393	0.97	24.60

Table 4.

S.No	[Complex] (in mol L^{-1})	[curcumin] (in mol L^{-1})	λ_{max} (nm)	$10^{-5}\varepsilon_{max}$	$10^{-1}K_b$
1.	2 X 10^{-4}	2 X 10^{-6}	412	10.51	5.64
2.	2 X 10^{-4}	4 X 10^{-6}	420	7.15	7.45
3.	2 X 10^{-4}	6 X 10^{-6}	420	6.28	8.68
4.	2 X 10^{-4}	8 X 10^{-6}	419	6.18	9.58
5.	2 X 10^{-4}	10 X 10^{-6}	419	6.02	10.10

Table. 5.

S.No	[Complex] (in mol L^{-1})	[curcumin] (in mol L^{-1})	λ_{max} (nm)	$10^{-6}\varepsilon_{max}$	$10^{-1}K_b$
1.	2X 10^{-4}	2 X 10^{-6}	440	2.80	2.00

2.	2×10^{-4}	4×10^{-6}	415	1.80	3.90
3.	2×10^{-4}	6×10^{-6}	417	1.40	5.30
4.	2×10^{-4}	8×10^{-6}	417	1.30	5.90

Table 6.

S.No	[Complex] (in mol L^{-1})	[curcumin] (in mol L^{-1})	λ_{max} (nm)	$10^{-5}\varepsilon_{max}$	$10^{-3}K_b$
1.	2×10^{-4}	2×10^{-6}	453	9.47	4.25
2.	2×10^{-4}	4×10^{-6}	444	7.59	4.70
3.	2×10^{-4}	6×10^{-6}	435	7.38	4.72
4.	2×10^{-4}	8×10^{-6}	432	7.13	4.79
5.	2×10^{-4}	10×10^{-6}	428	6.69	4.84
6.	2×10^{-4}	12×10^{-6}	427	6.88	4.89
7.	2×10^{-4}	14×10^{-6}	426	7.04	4.92

Table 7.

S.No	[Complex] (in mol L^{-1})	[curcumin] (in mol L^{-1})	λ_{max} (nm)	$10^{-5}\varepsilon_{max}$	$10^{-3}K_b$
1.	2×10^{-4}	2×10^{-6}	394	29.64	4.61
2.	2×10^{-4}	4×10^{-6}	419	2.90	3.02
3.	2×10^{-4}	6×10^{-6}	422	2.73	3.57
4.	2×10^{-4}	8×10^{-6}	423	2.73	3.95
5.	2×10^{-4}	10×10^{-6}	424	2.53	4.10
6.	2×10^{-4}	12×10^{-6}	425	2.44	4.24
7.	2×10^{-4}	14×10^{-6}	425	2.49	4.40

Table 8.

S.No	[Complex] (in mol L^{-1})	[curcumin] (in mol L^{-1})	λ_{max} (nm)	$10^{-5}\varepsilon_{max}$	$10^{-3}K_b$
1.	2×10^{-4}	2×10^{-6}	412	10.88	2.64
2.	2×10^{-4}	4×10^{-6}	412	7.39	3.28
3.	2×10^{-4}	6×10^{-6}	414	7.37	3.86
4.	2×10^{-4}	8×10^{-6}	414	7.17	4.02
5.	2×10^{-4}	10×10^{-6}	415	6.78	4.29
6.	2×10^{-4}	12×10^{-6}	416	6.54	4.42
7.	2×10^{-4}	14×10^{-6}	416	6.39	4.50

Figure Captions:
Figure 1. Structure of Metal-Salen complexes (I-VI) and Curcumin.
Figure 2. Electronic absorption spectrum of complex 4 (left) and curcumin (right) in acetonitrile at 298 K.
Figure 3. Overlay electronic absorption spectrum of complex 4 during incremental addition of curcumin in acetonitrile at 298 K.
Table Captions:
Table 1. The LMCT absorption maximum and electrochemical data of complexes (1-6) in acetonitrile at 298 K.
Table 2. IR Spectral data of Metal- salen Complexes in acetonirile at 298 K.
Table 3. UV-visible titration of Fe -salen Complex 1 with curcumin and binding constants at 298 K.
Table 4. UV-visible titration of Fe-chloro salen Complex 2 with curcumin and binding constants at 298 K.
Table 5. UV-visible titration of $Fe(Me)_2$ Salen Complex 3 with curcumin and binding constants at 298 K.
Table 6. UV-visible titration of $Fe(NO_2)_2$ Salen Complex 4 with curcumin and binding constants at 298 K.
Table 7. UV-visible titration of Mn- Salen Complex 5 with curcumin and binding constants at 298 K.
Table 8. UV-visible titration of Chromium Salen Complex 6 with curcumin and binding constants at 298 K.

Supporting Informations:

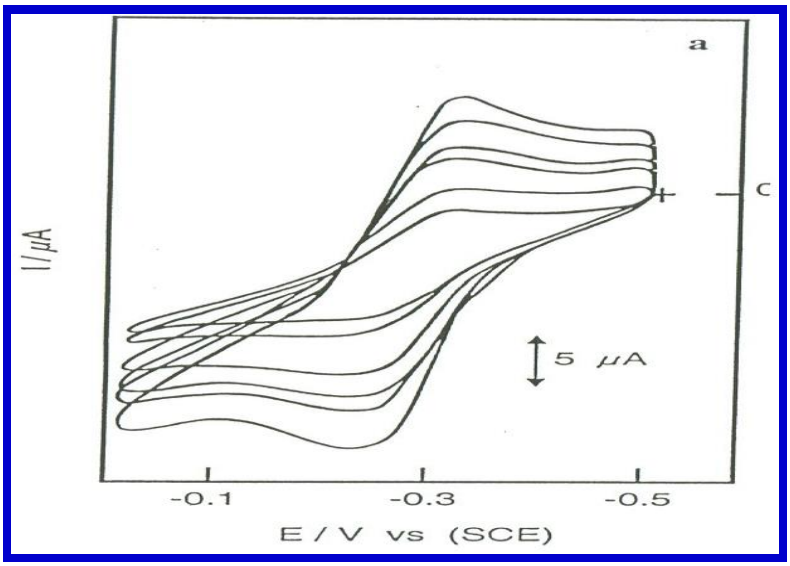

SI 1. Cyclic voltammogram of complex **1** at different scan rate.

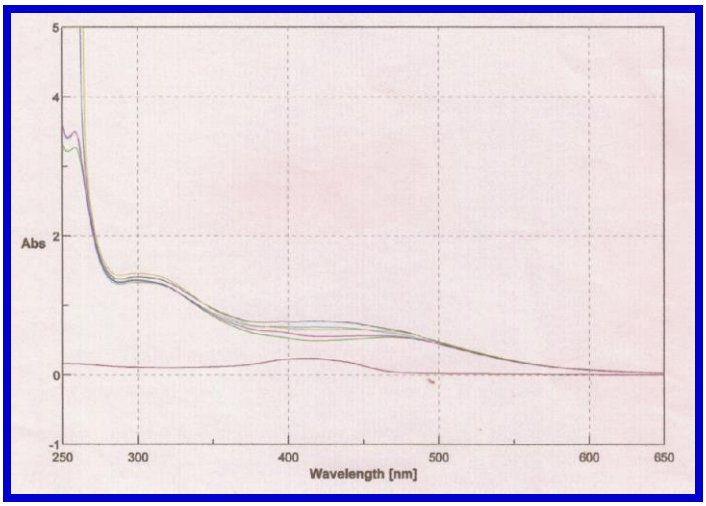

SI 2. Overlay electronic absorption spectrum of complex 1 during incremental addition of curcumin in acetonitrile at 298 K.

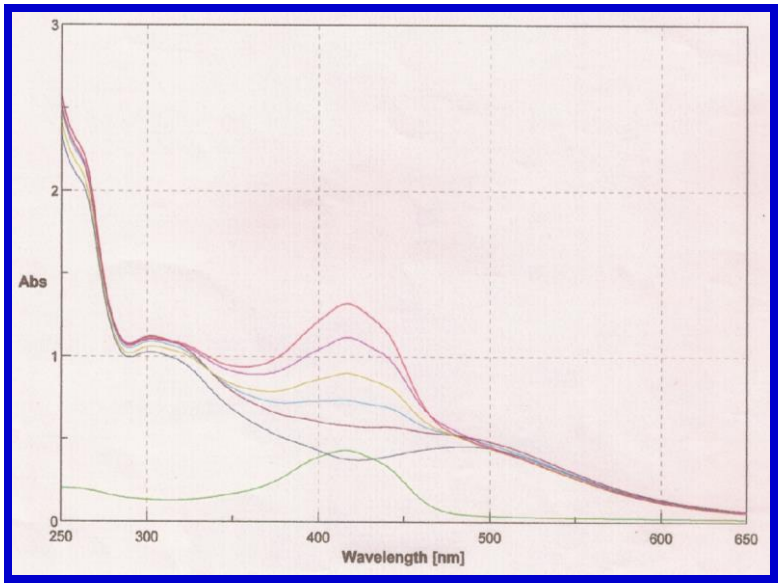

SI 3. Overlay electronic absorption spectrum of complex 3 during incremental addition of curcumin in acetonitrile at 298 K.

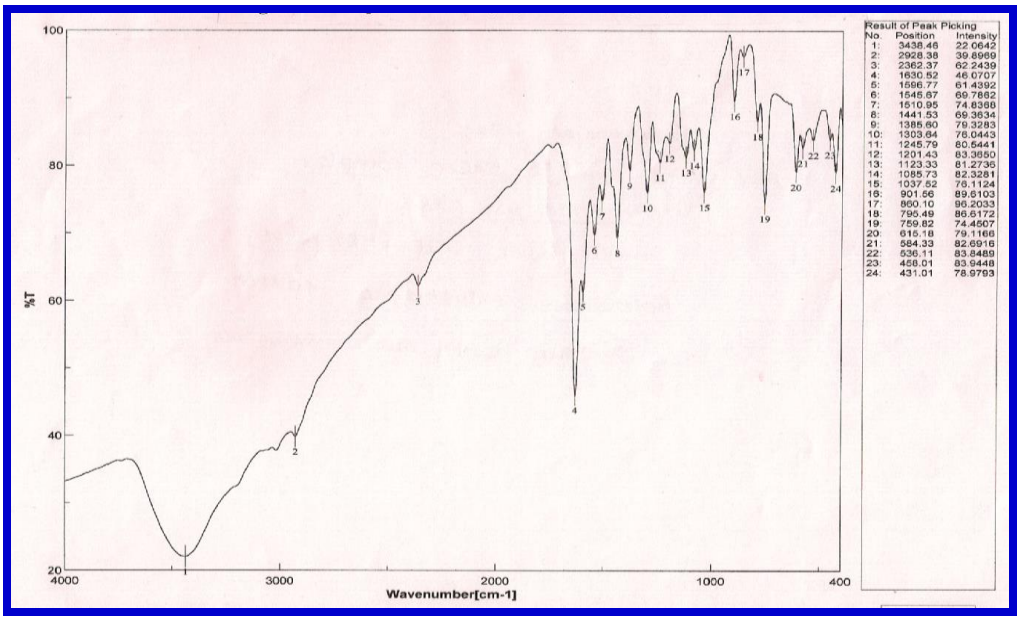

SI 4. FT-IR spectrum of complex 1 in acetonitrile at 298 K.

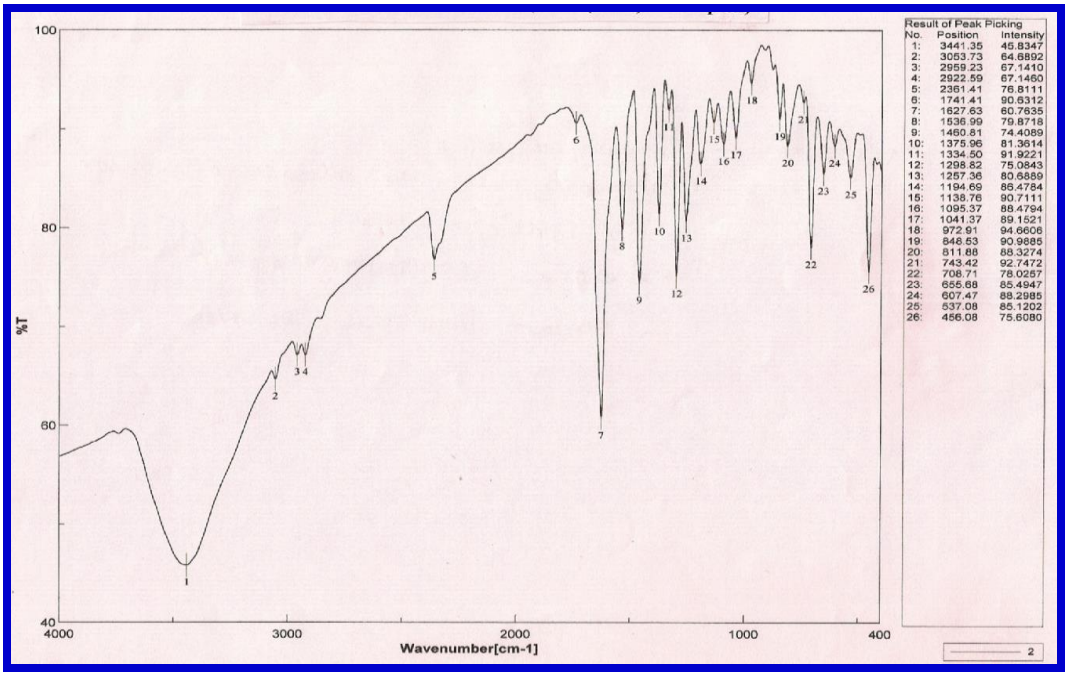

SI 5. FT-IR spectrum of complex 2 in acetonitrile at 298 K.

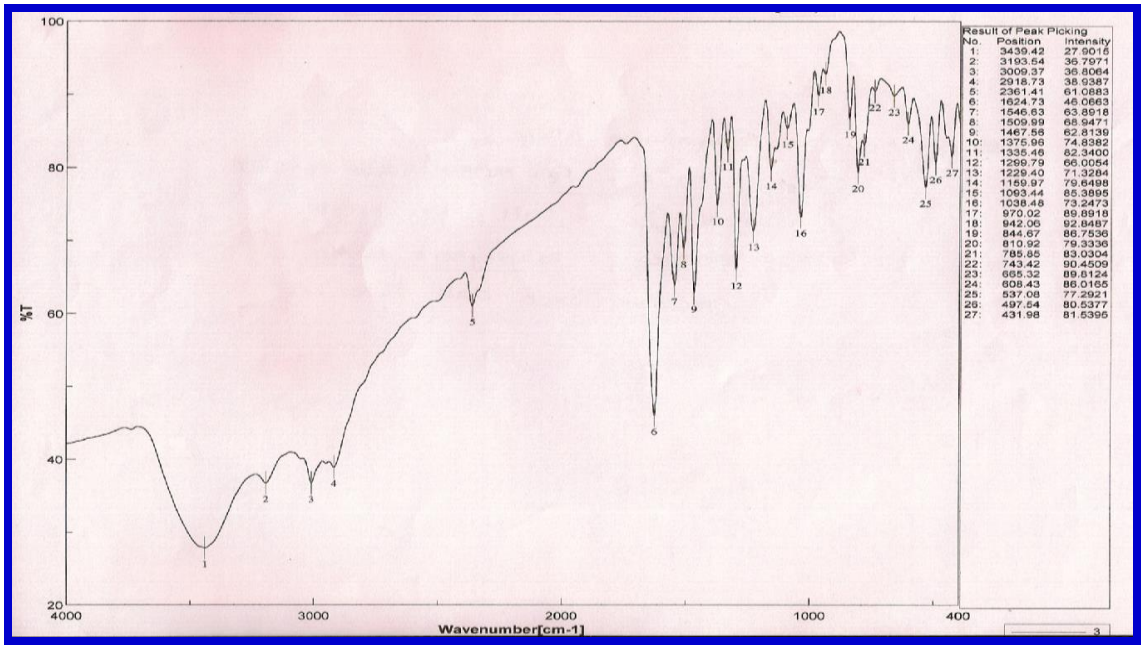

SI 6. FT-IR spectrum of complex 3 in acetonitrile at 298 K.